Published in final edited form as:
Cell Biochem Biophys. 2008 ; 52(1): 1–18. doi:10.1007/s12013-008-9024-5.

Mechanosensitive Channels: Insights from Continuum-Based Simulations

Yuye Tang[a], **Jejoong Yoo**[b], **Arun Yethiraj**[b], **Qiang Cui**[b,*], and **Xi Chen**[a,*]

a *Nanomechanics Research Center, Department of Civil Engineering and Engineering Mechanics, Columbia University, New York, NY 10027*

b *Theoretical Chemistry Institute, Department of Chemistry, University of Wisconsin, Madison, WI 53706*

Abstract

Mechanotransduction plays an important role in regulating cell functions and it is an active topic of research in biophysics. Despite recent advances in experimental and numerical techniques, the intrinsic multiscale nature imposes tremendous challenges for revealing the working mechanisms of mechanosensitive channels. Recently, a continuum-mechanics based hierarchical modeling and simulation framework has been established and applied to study the mechanical responses and gating behaviors of a prototypical mechanosensitive channel, the mechanosensitive channel of large conductance (MscL) in bacteria *Escherichia coli* (*E. coli*), from which several putative gating mechanisms have been tested and new insights deduced. This article reviews these latest findings using the continuum mechanics framework and suggests possible improvements for future simulation studies. This computationally efficient and versatile continuum-mechanics based protocol is poised to make contributions to the study of a variety of mechanobiology problems.

1 Introduction

Cellular mechanotransduction, which is the mechanism by which cells convert mechanical stimuli into biochemical responses, has been a research focus for several decades owing to its significance in many physiological functions in living organisms, such as touching, balance, and hearing, among others (1–4). In the larva of *Caenorhabditis elegans* (*C. elegans*), for instance, its movement is achieved through muscle contraction regulated by a three-neuron reflex circuit, in which gating of the membrane-bound Degenerin/Epithelial Sodium Channel (DEG/ENaC channel) is a key factor (5). Malfunction of any stage in the mechanotransduction pathway, such as mutations of MEC-4 or MEC-10 degenerins in the DEG/ENaC channel of the nematode, leads to touch insensitivity. Despite the significance of mechanotransduction, the detailed mechanisms by which the cell responses to external stimuli are not yet well understood.

During mechanotransduction, the external force at macroscopic scale can transcend down multiple length scales to affect the microscopic mechanical behaviors of biomolecules and their assemblies. Therefore, understanding the molecular basis for mechanotransduction requires bridging multiple length- and timescales along with an efficient treatment of the complex structure of biomolecules; this is still challenging for experimental studies, and thus important insights are sought from modeling and simulations. The present numerical schemes based on all-atom simulations are limited to simple loading modes occurring at nanometer scales and nanosecond events. An efficient multiscale framework that can both capture

*Corresponding authors. E-mail address: cui@chem.wisc.edu (Q. Cui) and xichen@civil.columbia.edu (X. Chen).

sufficient molecular details and deal with complex loadings over multiple scales is undoubtedly a valuable supplement to the standard experimental and modeling methods. In our recent studies (6–8), we have developed a top-down approach that effectively models the biomolecules and their assemblies as integrated structures as an attempt to bridge the aforementioned gap, allowing physical mechanistic insights of mechanotransduction to be deduced.

Using the representative system of *E. coli*-MscL as the example, current understandings of mechanotransduction based on experimental analysis, theoretical modeling and numerical simulations are reviewed in this paper. Since a set of up-to-date and extensive reviews has been recently published on the experimental studies of MS channels in volumes 58 and 59 of *Current Topics in Membrane*, we will mainly focus on the computational aspects, especially insights regarding MscL using our own continuum-based framework (6–8). We believe that many of these insights are highly relevant in the analysis of a host of other biomolecular systems, such as the mechanosensitive (MS) channels in higher organisms. Further improvements of this multiscale model are also discussed and it is envisioned that such a refined framework will find great value in the study of mechanobiology.

2. Overview of Mechanosensitive (MS) Channels

Although some long-term mechanotransduction events such as tissue remodeling involve the consequence of the altered gene expression, most cellular responses to mechanical forces are due to the MS channels (1,4,9). Besides the DEG/ENaC channels mentioned earlier, there exists many other families of MS channels with diverse functions and gating mechanisms. For example, the transient receptor potential (TRP) channels play an important role in the auditory transduction and amplification of *Drosophila* by ciliary movements (10); some G protein-coupled receptors (GPCR) serve as mechanosensors for fluid shear stress and they are critical to tissue repairing and wound healing (11). Despite the key physiological functions of these eukaryotic MS channels, little is known about their working mechanisms. Most mechanistic insights have been collected via studies of their homologs in bacteria, some of which have been structurally characterized by moderate-resolution (~3 Å) X-ray crystallography (12) or homology models (13).

In bacteria, MS channels respond to load perturbation applied to the cell membrane or other membrane-associated components and act as “safety valves” by allowing permeation of small ions and water molecules at high osmotic pressure (4). So far, one of the most studied MS channels is *E. coli*-MscL, which has been chosen as a model system thanks to its ubiquity and simpler structure. In Figure 1a/b (top/side views), the structure of *E. coli*-MscL in the closed state is shown, which was developed by homology modeling (13–15) based on the *X*-ray crystal structure of MscL in bacteria *Mycobacterium Tuberculosis* (*Tb*) (12) and available experimental constraints (16). The structure of *E. coli*-MscL is of five-fold symmetry, and the residues on top of the transmembrane helices are connected by periplasmic loops (black), whereas those at the bottom of the transmembrane helices are linked to cytoplasmic helices via cytoplasmic loops (black). Among the transmembrane helices that directly interact with the membrane, the TM1 bundle (sky blue) consists of five longer helices that form an inner gate, and the five TM2 helices (yellow) form the outer bundle. The dash line in Figure 1b indicates the approximate location of lipid membrane. In *E. coli*-MscL, TM1 and TM2 helices correspond to residues Asn 15-Gly 50 and Val 77-Glu 107, respectively. There is a break in TM1 due to Pro43 (red) near the top of the TM1 helix, and in the literature, the segment above Pro43 is sometimes referred to as the S2 helices (13). The cytoplasmic domain is composed of bundles formed by S1 helices (green) and S3 helices (grey), which correspond to residues Ile 3-Met 12 and Lys 117-Arg 135, respectively. Note that the configurations of the S3 helices are different in the homology models in ref. (15) and ref. (14), where the S3 helices are longer

in the newer model; in this paper we use the structure described in ref. (14) as the closed configuration. Among the three inner helical assemblies formed by the TM1, S1 and S3 helix bundles, the transmembrane pore enclosed by TM1 helices is the most important and determines the ion flux that passes through; the size of the pore can be estimated by measuring the electric current experimentally (16). An effective radius of the channel can be calculated from the area of the pentagon projection on the membrane plane formed by the principle axes of the TM1 helix bundle, which is ~6.5Å for the *E. coli*-MscL in its closed state.

The gating transitions of MS channels are triggered by external stimuli through their lipid environments. Membrane-activated gating behaviors were first observed by Kung's group by carrying out patch-clamp experiments on lipid vesicles (17); since cytoskeleton and other membrane proteins were removed *a priori*, the mechanical deformation of lipid was demonstrated to be important during MS channel gating. The crucial role of membrane was also emphasized based on a thermodynamics analysis (18), where the free-energy of the lipid bilayer deformation was estimated to be on the same order of magnitude as the energy barrier required for gating. Other experiments (19–21) and numerical studies (22,23) showed that MS channels are sensitive to lipid composition. Therefore, a proper analysis of the gating of MS channels requires explicit consideration of the lipid membrane.

A lipid bilayer membrane is composed of phospholipids and it forms a natural barrier between the inside and outside of the cell to control materials exchange (24). The exposed head groups of phospholipids are hydrophilic, and the tails are hydrophobic toward the center of lipid bilayer. An example of dilauroyl-phosphatidylethanolamine (DLPE) lipid is shown in Figure 2a, in which an *E. coli*-MscL is inserted. Under the physiological condition, the lipid is usually found in the fluidic phase where it is incapable of bearing shear stress and cannot sustain large strains; several percent of area expansion may rupture the membrane (1). Nevertheless, within an elastic/viscoelastic framework, the effective mechanical properties of lipid (upon tension, bending, etc.) can be estimated through relevant loads and deformation perturbations, and used for modeling purposes (18). For instance, the area expansion coefficient of a lipid bilayer is the membrane tension per relative change of its unit area, which is related to an effective Young's modulus of the membrane. Lipid membrane is nearly incompressible (25), which implies an effective Poisson's ratio close to 0.5. Besides in-plane tension, bending of lipid bilayer affects its curvature, and this contribution from an effective bending stiffness has been suggested to be important for the gating of MS channels (26). The lipid property is inhomogeneous across the thickness and distinct peaks of lateral pressure have been characterized in the head group and tail regions as the area of the lipid is changed (22,27); modification of the pressure profile can lead to different channel gating characteristics (28–31).

A living cell is subjected to diverse external stimuli (1) including but not limited to steady-state contacts, high-frequency vibrations, fluid shear stresses, etc.; these external stimuli may be superimposed with those generated internally, such as cytoskeletal polymerization, osmotic and hemodynamic pressure. It is interesting to investigate which stimulus is more relevant to mechanotransduction pathways. Since the forces acting on a MS channel are transferred through the lipid, the effect of various membrane deformation modes (e.g., in-plane tension, bending, etc.) on the gating transition ought to be explored. The schematic in Figure 2a shows the example of equi-biaxial tension, which is the most studied membrane deformation mode that can be triggered by variation of the osmotic pressure.

3. Previous Studies of MscL

3.1. Previous experimental investigations

Patch clamp experiments have been a major tool for exploring the mechanism of cellular mechanotransduction. MS channels in the bacterial spheroplasts of *E. coli* were discovered by Martinac et al. (32) using this technique, which revealed pressure-activated, voltage dependent and ion selective properties. By electrophysiological characterization, the gating behaviors of *E. coli*-MscL were also observed in reconstituted lipid vesicles (17). The relationship between channel opening probabilities and membrane tension was reported for MscL in (33) and a five-subconductance-states model was established, which showed that the tension-dependent conformational transition is primarily attributed to the pore area variation that occurred between the closed state and the first subconductance state (16).

Successful cloning and purification of *Tb*-MscL led to useful protein crystals and solution of the X-ray structure at moderate resolution (~3 Å) for the closed state. The availability of this structure was instrumental to the development of the homology model of *E. coli*-MscL and guided many mutagenesis studies; it also made it possible to carry out atomistic simulations to explore the mechanism of MscL. Nevertheless, it is worth emphasizing that due to the difference between crystallization and physiological conditions, X-ray structures of membrane proteins may not correspond to their functional state (also see Sect. 6.2), not to mention the technical challenges associated with the refinement of X-ray structures at moderate resolution. In the originally refined MscL structure (PDB code 1MSL), for example, the C-terminal S3 helix bundle adopts the unusual feature that hydrophobic groups face outwards while several negatively charged residues cluster together. Anishkin et al. (34) modified this part of the structure based on the structure of pentameric cartilage protein, and the resulting conformation was shown to be consistent with disulfide trapping experiments; a revision of the X-ray structure (PDB code 2OAR; (35,36).) also supports the new conformation of S3. Recently, the modified model has been confirmed by Maurer et al. (37) using combined computational and mutation studies. In a separate mutation study, Kloda et al. (38) showed that the orientation of the C-terminal S3 helix bundle is likely pH dependent, and a RKKEE cluster in that region in fact might function as a pH sensor.

The importance of various residues has been probed with numerous mutation studies. For example, the potential functional regions of MscL were revealed to involve Glu 56 and Lys 31 (39); Gly 14 may serve as a pivot for the “swing-like” motion of the N-terminus (40); the hydrophobicity of residue Gly 22, which locates at the narrowest part of *E. coli*-MscL, was shown to play an important role for pressure sensitivity (41). Loss-of-function mutations (42) found that the most severe mutations involve hydrophobic-to-hydrophilic substitutions at the rim of the funnel in MscL, which confirmed the idea that MscL receives forces from the membrane at the rim. Analysis of several gain-of-function mutants (e.g., V23D (43)) illustrated that the transition from the dehydrated state to the water-filled state of the pore is likely the rate-limiting step in the gating of wild type MscL, emphasizing that protein solvation could contribute substantially to the energetics of the gating process. Cutting or mutation of the periplasmic loops, especially the residues that face the membrane, facilitates the channel opening (44,45). Taken together, these results paint a mechanistic picture in which the gating energetics are due to the combination of protein hydration, elastic loops rearrangements and surrounding lipid membrane deformation.

Based on experimental constraints and known structural features of the transmembrane proteins, structural models for the gating transition of *Tb*-MscL and *E. coli*-MscL upon equi-biaxial tension have been proposed (15). These models include 13 conformational states ranging from the closed state (with the effective pore radius, a, of about 6.5 Å) to an open conformation (when the maximum conductance can be measured experimentally) with a=19

Å; these structural models are consistent with the results from cysteine cross-linking experiments (13). Subsequently, structural rearrangements in the large prokaryotic MscL were determined by Perozo and co-workers (20,46) using electron paramagnetic resonance spectroscopy (EPR) and site-directed spin labeling (SDSL). The diameter change of the channel pentamer between its closed and open states was also characterized by a fluorescence resonance energy transfer (FRET) spectroscopic analysis (47). Although tilts and rotation of transmembrane helices are features in the models of both Sukharev et al. (15) and Porozo et al. (35), the magnitude of TM1 rotation is very different; the degree of TM1 rotation is counterclock wise (viewing from the cytoplasmic side) and slight in (15), while the rotation is 110° clockwise in (35). More recent *in vivo* SCAM (substituted cystein accessibility method) (48) and metal binding assays seem to be more consistent with the model based on EPR studies (35).

3.2. Previous Analytical Modeling Efforts

Theoretical studies are useful for postulating the principles behind the gating transition of MscL. A gating-by-tilting model was proposed based on thermodynamics as an alternative mechanism for dilatational gating (26). By considering possible deformation mechanisms (e.g. membrane tension and torque), a thermodynamics formulation was presented by Philips et al., who established a pioneering lipid-centric model (18) where the system energy is dominated by hydrophobic mismatch and lipid tension while ignoring the contribution from protein deformation. This model was improved by incorporating other triggers, such as the change of membrane curvature and mid-plane deformation between the closed and open states (31); more recently, the model was further extended to study gating co-operativity (49).

Although these thermodynamics-based models have provided useful insights into the common features of MS channels, the lack of sufficient structural details makes it difficult to evaluate their validity for a specific system (which is particularly important in biological systems where certain atomistic features are crucial to structure and function). For example, the proteins were treated as either rigid or overly simplified objects (18,31,49), and thus their deformation energy contributions were largely ignored. Moreover, key parameters in these models were usually not derived from detailed simulations or experiments.

The elastic network model (ENM) (50) is a useful and efficient analytical alternative that incorporates the most salient structural details of the protein. In ENM, the atomic structure of a macromolecule is simplified as a network of elastic springs, where a harmonic spring is applied to any pair of atoms (often C α only) within a specified cut-off distance. Numerous studies have shown that ENM can reliably reproduce low-frequency modes of proteins, which are often highly correlated to functional transitions. For MscL in particular, Valadie et al. (51) showed that the conformational transitions among the first few structures in the model of Sukharev et al. (15) can be described with three low-frequency modes only. The character of these modes clearly indicates an iris-like movement involving both tilt and twist rotation of the transmembrane helices. The low-frequency modes can also be used in a linear-response framework (52) to predict structural changes upon pulling force from the membrane. For *E. coli*-MscL, the structural changes upon equi-biaxial tension predicted by ENM (8) agreed qualitatively with structural models (14). This protocol, however, requires explicit force or displacement boundary conditions applied on certain atoms, which are not straightforward to select (7,8).

3.3. Previous Numerical Approaches

Numerical simulation is a powerful approach for exploring the fundamental principles of mechanobiology. Comparing with analytical modeling, numerical simulations can incorporate sufficient structural details to propose or verify various mechanistic hypotheses as well as to

improve the model. In addition, numerical experiments can be manipulated in a well-defined way to help both interpret existing experimental data and design or stimulate new experiments.

All-atom simulations based on molecular dynamics (MD) are in principle capable of depicting the gating transitions at the finest scale (53). However, they are prohibitively expensive especially when the protein, lipid membrane, and surrounding solvent are explicitly considered (54). MD simulation was first applied to study the gating of *Tb*-MscL (55); limited by the accessible time-scale (3ns), the pore size barely changed during the simulation. Another 20ns simulation resulted in a similar behavior where the pore remained closed (56). To accelerate structural transitions, the protein deformation was decoupled from the membrane, and external forces were applied directly to the protein so as to assist gating. The steered molecular dynamics (SMD) was used to study the *E. coli*-MscL upon equi-biaxial tension (54), where the steering forces, estimated from the lateral and normal pressure profiles exerted by the deformed bilayer (22), were added on selected boundary atoms of the protein. Despite this bias, the channel merely opened to a=9.4 Å after 12 ns of simulation, which highlights the limit of atomistic MD simulations in the context of probing the gating process. In fact, according to a recent work (56), in all-atom simulations the channel opening could be directly observed only when an explicit lateral bias force (in the radially outward direction) was applied to all five subunits of MscL.

Another artificially accelerated approach is the targeted MD (TMD) (57). In (58), the lipid bilayer membrane was completely ignored and a holonomic constraint was used to drive the opening of an *E. coli*-MscL. The constraining force, however, can be unrealistically large, which makes the targeted MD useful only in a qualitative sense. In general, the final open structure must be specified in TMD simulations (thus gating is guaranteed), which is another major limitation. A similar approach was carried out by Bilston and coworkers (59) on a *Tb*-MscL without explicit lipid membrane, where the opening of MscL was possible if the membrane tension was beyond 12 dyn/cm.

During simulations at short time-scale, the applied external forces can lead to unrealistic protein structural transitions and protein/lipid interactions. To partially circumvent this problem, inspired by the findings from experiments (20), Meyer et al. (60) studied the conformational transitions of *E. coli*-MscL in a pre-curved lipid membrane. Interesting observations were found through a 9.5 ns simulation, where the major structural rearrangements occurred in the periplamic loops and extracelluar helices. Although the channel radius increment was still limited, this technique has attempted to combine bending and equi-biaxial tension modes, and the transition of *E. coli*-MscL occurred locally in the absence of global external forces.

The effect of different lipids has been studied in several recent all-atom simulations of MscL. Elmore et al. (23) carried out simulations with MscL in several lipid bilayers with different headgroups and tails. Substituting lipid headgroup was found to modify protein-lipid interactions, which in turn led to different conformations of MscL. Changing the tail length and therefore the membrane thickness also induced structural changes in the channel. More recently, Debret et al. (61) compared simulations of MscL in DMPE and POPE, two lipids of different tail lengths. The MscL structure remained stable in the POPE simulations but the transmembrane helices underwent tilts and kinks in the thinner DMPE simulations. These observations confirmed the importance of hydrophobic mismatch in the gating process.

Despite various improvements, the all-atom-based simulations are still computationally intensive and the short simulation time may be inadequate for statistical sampling. Hence, developing coarse-grained models to access longer time scales has become an important topic in the simulation community (62–65). Most of the efforts have been focused on developing particle based models in which one bead represents a group of atoms. In the context of MscL,

building upon their success in developing an effective coarse-grained model for lipids, Marrink et al. developed a coarse-grained model (62) for MscL based on the transfer free energy of amino acids between water and lipid. The gating transition of MscL was successfully observed in the simulation, although still at elevated tension (60 mN/m rather than the experimental value of 20 mN/m required to open the wild type Tb-MscL) and temperature (338 K); moreover, the final open state accessed in the simulation has a pore somewhat smaller than estimated in the literature (radius of 0.7–0.75 nm vs. 1–2 nm). However, the coarse-grained model did reproduce the experimental observation that the V21D mutant opens at substantially lower tension than the WT, confirming the idea that solvation of hydrophobic residues constitutes an important part of the energy barrier for gating. With further improvements in the way that protein structures are described, the particle based coarse-graining framework is very promising, especially in terms of a physically transparent way to describe protein/lipid interactions.

Despite its great potential, particle based coarse-grained models still suffers from significant computational cost and it is still not routine to carry out multiple simulations to the millisecond scale, which is often the biologically relevant time scale. Moreover, in the specific context of mechanosensation and mechanotransduction, it is not straightforward to apply particle based models to study deformations involving large length scales or complex loading modes. These considerations motivated us to develop a continuum mechanics-based simulation framework for mechanobiology (7,8) that can potentially bridge multiple length scales and adapt complex loadings; at the same time, the model can include sufficient molecular details to capture some of the most important characteristics of a specific system. In the MDeFEM framework, the biomolecules and their assemblies are modeled as integrated continuum structures that maintain some of the most important structural details (and redundant atomic details are excluded). This is motivated by the observation that the mechanical deformation of a biomolecular system is dictated by the superposition of several of its lowest modes, which can be well described by the “collective” behavior of its structural motifs (via phenomenological mechanical properties) and most local chemical/atomistic details are less important. Thus, the aim of our MDeFEM approach is to efficiently treat deformations at large length scales and complex deformation modes inaccessible to conventional MD simulations, while retaining key features from atomistic simulations at various levels of sophistication.

In the following, we illustrate the MDeFEM model through discussions of its application to *E. coli*-MscL (Figure 2b) (7, 8). To focus on the key physical principles that govern the gating process, we limit ourselves to very simple models of the channel in these preliminary studies, bearing in mind that the model can be systematically improved in the future (see Sect. 6). We believe that many of the underlying physical principles that govern the gating of *E. coli*-MscL (8) are likely applicable to other mechanosensitive channels.

4. Continuum-based Approach: Model and Methods for Studying MscL

In Figure 1c/d, the top/side views of the continuum model of *E. coli*-MscL are shown (7); the geometries of all continuum components are measured from the closed state of the homology model (14) (Figure 1a/b). Each helix (TM1/TM2/S1/S2/S3) is modeled as a three-dimensional elastic cylinder with a diameter of 5 Å (a typical value for the main chain of an α-helix). As a first order approximation, the helix is taken to be homogeneous and isotropic, and the elastic properties remain constants during the gating transition. Due to its potentially important contribution, Pro43 (13) is treated in the helix model with an effective elastic modulus that is different from the rest part of TM1 helices. The loops are taken to be quasi-one dimensional elastic springs, whose mechanical properties are also assumed to be residue-independent. Effective materials properties, such as the nominal Young’s modulus and Poisson’s ratio of each helix and the spring constant of the loop, are calibrated by matching results of normal

mode analyses (with respect to several lowest eigenmodes and frequencies) at the atomistic and continuum levels (7).

At the simplest level, a lipid bilayer can be effectively modeled as a sandwich plate structure (Figure 2b) by considering the different roles played by the head and tail regions in transducing mechanical stress (22, 23). Each layer (head group or tail) is assumed to be homogeneous and elastic, whose effective thickness and elastic constants are fitted based on a previous MD study (22). To host the MS channel, a cavity with conforming shape is created in the membrane. Based on this continuum model, the assembled continuum structure of an *E. coli*-MscL inside a lipid bilayer is shown in Figure 2b.

In MDeFEM, the structural components of biomolecules are integrated together through non-bonded interactions, which represent electrostatic and van der Waals interactions. For simplicity, we do not distinguish these two types of interactions and the total non-bonded energy is assumed to obey an effective pair-wise potential function similar to the Lennard-Jones form, that is, $E_{\text{int}}(\alpha)=C\left[\frac{n}{m}\left(\frac{d_0}{\alpha}\right)^m-\left(\frac{d_0}{\alpha}\right)^n\right]$, where d_0 and α are the initial equilibrium distance and deformed distance between the two surfaces, respectively, and m and n denote the power indices for the repulsive and attractive terms, respectively, with $n < m$ in general. Using this particular functional form is clearly an approximation, although similar kinds of short-range effective interactions have been found appropriate in coarse-grained simulation of other condensed phase systems including highly polar liquids (66). Such non-bonded interactions are applied to all relevant pairs of surfaces in the due course of gating, thus, the "interaction areas" between objects do not change during deformation. The values of the "well-depth", C, and d_0, n, m, depend on different pairs of interactions (e.g. between helices and those between helix and lipid), and they are calibrated by calculating and matching potential energies at atomistic and continuum levels (7). Among the non-bonded interactions, the most essential one is the protein-lipid interaction; small perturbation of the corresponding C value has a negligible effect whereas a significant change (e.g. 50% reduction) of the C parameter leads to more difficult gating.

Parameterization of helices, loops, lipid, and interactions is described in ref. (7). These parameters are meant to be order-of-magnitude estimates, and more quantitative parameterization (which also includes the functional form of non-bonded interactions) is an essential aspect for refinement in the future, see Section 6. The integrated system is meshed with finite elements (see example in Figure 1e for the mesh of protein bundle and Figure 2b for the elements near lipid cavity). Commercial software ABAQUS (67) is used for FEM analyses. By taking advantage of the continuum approach, the typical simulation time is only a few hours on a regular workstation with a single CPU.

5. Gating Mechanisms of MscL and Insights for Mechanotransduction

5.1. Effect of different loading modes

In previous experimental and theoretical studies (20,26,30,31,33,54,56,60), several loading modes have been postulated to be the trigger of MscL gating, including dilatational gating (equi-biaxial tension) and gating-by-tilting (axisymmetric bending). These potential gating mechanisms are examined with MDeFEM simulations (8) to explore mechanotransduction pathways under different deformation modes.

5.1.1. Gating behaviors upon equi-biaxial tension—An equi-biaxial strain up to 21% has been applied as a displacement boundary condition on the membrane (8). Such a large strain is required due to modeling the lipid as a solid slab; despite such bias, an appropriate expansion of lipid cavity can be achieved, which is necessary to accommodate the fully opened

channel and appropriate for exploring the important aspects of the protein structural transition during gating.

The snap shots of the structural transition of *E. coli*-MscL at intermediate (half-opened) and open states obtained from MDeFEM (8) are given in Figure 3; compared to the structural model (14) they show good agreement, which is encouraging considering the numerous approximations made in our model (see further discussions below). It is not surprising that with the increase of membrane strain, the lipid cavity expands and the forces are transmitted to the transmembrane helices of the protein structure via non-bonded interactions. Consequently, the transmembrane region undergoes most conformational changes characterized by their radial expansions, and the pore enclosed by the TM1 bundle opens up.

Besides the lateral expansion, visible shrinking in the thickness is also observed for the transmembrane region, which is correlated with significant tilting of the helices. The longer and more flexible TM1 bends more than TM2 helices – such significant deformation, which is required to maintain mechanical equilibrium during the gating process (8), remains to be verified from experimental studies with sufficient resolution (we note that the structural model (14) also predicted significant helix bending curvature, Figure 3).

The MscL pore is defined by the TM1 helices; thus the loops connecting TM1 and TM2 helices also impose constraints on the size of the pore. In addition, the S1 helices affect the pore conformation via interaction with TM1 helices; during gating, the S1 bundle expands in the radial direction and are lifted up towards the transmembrane region, which confirms the "swing-like" motions of the N-terminus (40). The expansion of the S1 helices, however, is smaller than in the structural model, which might be caused by the neglect of solvation contributions in the current model (see Section 6). Being far away from the transmembrane helices, the S3 assembly remains essentially unchanged – this finding is in agreement with the later version of the structural model (14) (as opposed to the previous version (15)), suggesting that the S3 helices are less important in terms of their mechanics roles (although they may bear other biochemical functions). The present system is resilient and can recover its closed state when the membrane stress is removed.

In Figure 4a, the percentage increment of the effective pore radius of *E. coli*-MscL, a, is calculated from MDeFEM simulation as a function of membrane strain (the open-square curve) (8). According to elasticity, the relationship between membrane strain and lipid cavity expansion is linear (7), which leads to the monotonic behavior of pore radius increment; the small deviation from perfect linearity in Figure 4a is due to the many-body interactions that affect equilibrium. At small strain, the variation of channel radius agrees well between MDeFEM (8) and SMD simulations (the open-circle curve in Figure 4a) (54). This demonstrates that at least qualitatively, the continuum-based model has a reasonable description for the forces involved in the gating process.

Another parameter characterizing the pore shape variation is the averaged tilting angle of TM1 helices (with respect to the membrane plane), which decreases monotonically with pore radius (open-square curve in Figure 4b) (8). Again, the MDeFEM results agree qualitatively with the structural model in the intermediate and open states (solid-diamond symbols) (14). We note that the MDeFEM simulations are based only upon the closed structure of MscL (unlike that in many other simulations where the final state must also be given so as to explore the pathways in between (58)), and thus such agreement is quite remarkable considering the preliminary nature of our model. As mentioned in Sect.3, the mechanistic model of Sukharev et al. (15) differs from that of Porozo et al. (35) regarding the rotation of the TM1 helices. Since there is no sidechain in the preliminary MDeFEM model, it is difficult to distinguish the two

mechanistic proposals at this stage; this remains an interesting subject for future MDeFEM study that employs more realistic shape for the continuum components.

Although the MDeFEM study has demonstrated some promising results and agreements with the structural model, the rather monotonic behaviors of pore radius and helix tilting angle in Figure 4 illustrates a main limitation of the current continuum model, in which the effective (free) energy surface is essentially downhill towards the open state in the presence of external load. This is inconsistent with the free energy profile estimated in ref. (16), which involves various intermediate states separated by pronounced free energy barriers; moreover, in the open state, the channel radius is essentially insensitive to a wide range of tensions in experiments. We believe that further refinements, such as incorporating the effect of solvation forces (43, 62,68), may help to make the MDeFEM approach more realistic (see Section 6). Indeed, analysis of gain-of-function mutants (43) suggested that the unfavorable solvation of hydrophobic residues that line the channel pore constitutes a major part of the energy barrier for gating.

5.1.2. Gating behaviors upon bending—Membrane bending is a commonly encountered deformation mode in a flexible cellular structure, and becomes prominent during cell adhesion/contact. In order to study the pure bending behavior (i.e., decouple with membrane stretching), a four-point bend flexure of a circular membrane has been studied (8). With respect to the insert in Figure 5a, one can define the cone angle, β, with reference to the effective radii of the five TM1 helices at the locations that correspond to the surfaces of the lipid membrane. When the membrane is bent upwards, the cone angle decreases almost monotonically with bending moment, and the TM1 helices become more upright at the final stage (Figure 5a).

Whether pure bending is an effective mode to promote gating can be explored from the effective pore radius evolution with bending moment (Figure 5b). Despite the wall rotation of the lipid cavity, the average cavity radius throughout thickness remains about the same during pure bending; therefore, the overall variation of the channel radius is small. The snapshots of the channel at half and maximum bending moment are also given in Figure 5b, where it is shown that despite the protein conformational change, the transmembrane pore radius is only moderately enlarged. The evolution of pore radius shows a zigzag pathway with bending moment, which is attributed to the many-body interactions among the helices. Overall, without the stretching component, pure bending is not an effective mode to gate the channel. If excessive bending could occur and couple with significant in-plane stretching (20, 31, 60), the curvature effect can become important.

5.1.3. Insights of loading modes vs. mechanotransduction—When an equi-biaxial tension is applied on the membrane, gating is realized primarily by the iris-like expansion of TM1/TM2 helices in the radial direction, as well as tilting of the subunits, whose conformation transitions are directly coupled to the lipid deformation. The S1 pore is also pulled open, in part due to its non-bonded interactions with the transmembrane helices, and in part because of the loop “linkers”. The conformational transitions of the intermediate and open structures obtained from the MDeFEM simulation are qualitatively similar to the structural models (14). In addition, the simulation results match with all-atom steered MD computations(54) regarding the channel radius evolution at the initial stage of the gating transition (Fig. 4a). These observations indicate that the gating process is dominated by mechanics principles, including lipid membrane deformation and the deformation/interaction of the helices/loops.

The bending mode has been shown to only slightly affect the overall channel radius. Thus, channel gating is relevant to some basic deformation modes (e.g. equi-biaxial tension) in the membrane but not others (e.g. pure bending). Other deformation modes have also been studied (8) and from the mechanistic point of view, equi-biaxial tension is the most efficient way to

achieve full gating. When these basic modes are combined, such as bending coupled with tension, the contribution of bending (membrane curvature) can be important for conformational transitions of the protein.

The present study deals with "external" load acted on the membrane only. In fact, during gating when the hydrophobic residues of the protein are exposed to water, the solvation force that generated "internally" can also play an important role in destabilizing specific conformations and affect gating (68). This important contribution is missing in the present MDeFEM approach (see discussions below on future improvements). Thus, the present agreement between MDeFEM and previous experimental and numerical studies may be in part due to error cancellation.

5.2. Effects of structural motifs

One of the focal points of biophysical studies of mechanotransduction is to understand the diverse roles played by different structural components, such as the helices and loops in MS channels (14,15). To that end, one may remove individual group of structural motifs (8) and explore the change in gating behaviors. Since equi-biaxial tension is shown to be the most effective for opening the MS channel, in the following we focus on this basic loading mode. The membrane strain is controlled at 21%, which is required for maximum gating for the complete (reference) protein model shown in Figure 6a.

In Figure 6b (8), upon removal of the loops connecting TM1 and TM2 helices, the constraining effect is reduced and the averaged TM1 tilting angle is decreased by about 10° in the final state. The bending curvature of TM1 and TM2 helices also seems to be increased, which further affects the shapes of S1 and S3 bundles. Thus, the periplasmic loops are moderately important. This observation can be compared to the experimental finding that cutting the periplasmic loops facilitated the gating transition (44, 45), although our "loopless" model is an oversimplification to the experimental system, in which the periplasmic loops were cut but not removed. Nevertheless, the qualitative behaviors are consistent.

Removing the S3 helix bundle has an insignificant effect on the deformation of the TM1/TM2/S1 helices (Figure 6c) (8), which is consistent with recent experiments (34); this is because S3 helices are far away from the other transmembrane protein components. When all structural components are kept except the loops that connect TM1 and S1 helices, the S1 pore becomes distorted, which in turn affects both TM1 and TM2 helices (Figure 6d) (8), illustrating the importance of these loops and the S1 bundle. These findings are in qualitative agreement with experimental observations (15).

These trends are quantitatively shown in Figures 4a and 4b. After the S3 helices are removed, both the evolutions of pore radius and the TM1 helix tilting angle are almost identical to those found with the full protein model; as the loops (either TM1/TM2 or S1/TM1 linker) are taken away, the reduced constraining effect leads to a wider pore in the opened state (8). These results show that during gating, different protein components bear diverse mechanical functions. The loops between TM1-TM2 helices and the loops between TM1-S1 helices, for example, may moderately affect the configuration of the channel in the fully open state. The most important helical components are the transmembrane helices, which directly interact with the membrane and "sense" the forces. These findings (8) are consistent with discussions in previous studies (15, 34) and again illustrate the underlying mechanical principles for MscL gating.

5.3. Co-operativity of MS channels

Biological membranes are highly heterogeneous and rich in proteins and other biomolecular components such as polysaccharides. Consider the most fundamental cooperativity problem

where two MscLs are spatially close to each other (8). The configurations of the channel at membrane strain of 21% are given in Figure 7 as the center-to-center separation between the MscLs is varied. When the two proteins are separated far apart, they do not affect each other's conformation. When the separation is reduced to 90 Å, the first column of Figure 7 shows that the TM1 pore becomes slightly distorted (with respect to that shown in Figure 3 or Figure 6a), which implies that the MscL starts to sense the existence of its neighbor. As the two channels further approach each other (with a separation 60 Å), the second column of Figure 7 demonstrates that the TM1 pore becomes more elliptical, indicating that the inter-channel interaction is significant.

In order to determine the critical distance at which co-operativity starts to occur, in Figure 8 we plot the bias ratio of the pore (the ratio between the shortest and longest axis) at maximum membrane strain as a function of channel separation. When the two channels are far apart, the bias ratio is 1. The bias ratio decreases gradually with separation, and when the channel center-to-center distance λ falls below about 100 Å, the reduction of the bias ratio is more significant – this leads to a critical separation of about 100 Å (8), which is roughly 4 times the radius of the undeformed lipid cavity (c). This finding is consistent with the simple mechanics analysis based on lipid elastic deformation: according to the plane stress solution (69), the normalized stress concentration factor of a plate containing two circular holes is increased sharply when the distance between these two holes is below about 4 times the hole radius (shown as open-square curve in Figure 8) – this critical separation is close to that identified from MDeFEM simulation. The critical separation of 100 Å is also consistent with that found by Ursell et al. (49). Thus, at a phenomenological level, the underlying mechanics principles provide a physical basis for MS channel co-operativity, although the quantitative aspects may depend on other physical and chemical features of the biological membrane and MS channels.

In (49), Ursell et al. used a lipid-centric mechanics model and found that the total membrane energy containing two "open" channels can be reduced when they are close to each other. Note that the protein deformation free energy and structural distortion were not considered in their model (49), thus whether such co-operative gating is realistic remains to be verified. The MDeFEM-based approach (8) further reveals that the pore shape can be significantly distorted due to channel-channel interaction, a feature that can be observed only with a model that includes structural details for the protein. To test this prediction, a carefully designed channel recording study can be employed to measure the current through each channel as a function of channel density.

5.4. Large scale simulations of lab experiments

The advantage of the MDeFEM framework is further demonstrated via the simulation of large scale experiments (8), such as the patch clamp experiments (16,17,33) that have been instrumental to the mechanistic analysis of mechanotransduction. From experiment (16), the geometry of the relatively rigid pipette can be measured (Figure 9a) and the opening of the pipette is 1 μm. Frictionless contact is assumed between the vesicle and pipette, which does not correspond to the tight-seal condition in many experiments *(70–72)* but can be improved without much difficulty; the change of such boundary condition could affect the required suction pressure for gating (although the required local membrane strain is still the same). Without losing generality, the lipid vesicle may be modeled as an impermeable shell (33) filled with cytoplasm with a bulk modulus same as pure water (2.2 GPa) (73). The averaged size of the liposome used in the patch clamp experiment in (33) was about 5 μm. To facilitate gating as well as to simplify the analysis, one can assume that an *E. coli*-MscL is located at the north pole of the vesicle (8), which leads to an equi-biaxial stress field and makes the problem axisymmetric.

Figure 9a illustrates the undeformed and deformed liposome configurations. By applying a suction pressure, the top portion of the vesicle membrane is attracted into the pipette and forms a bulge shape. The stress is also increased nonlinearly with the suction pressure; at about 0.7 bar of pressure, the local stress near the channel leads to MscL pore opening that is close to full gating (Figure 9b). The results also qualitatively agree with that measured from experiments (8, 16). The configuration of the final state of the channel is very close to that upon equi-biaxial tension on a flat membrane (Figure 3); this is to be expected since the pipette opening is much larger than the protein dimension.

These types of numerical simulations of lab experiments at the cellular scale clearly demonstrate the unique value of the multiscale approach. The versatile continuum-based simulation framework may explain, guide, and stimulate new experiments, where the protein location, number, species, and vesicle geometry can be varied. For example, spheroidal or ellipsoidal vesicle geometries can be used, and the resulting membrane tension stress will depend on the principal curvatures. Under such circumstance, the change of MscL location will lead to different gating behaviors including a distorted open pore; such characteristics can be revealed from carefully designed channel recording experiments. In addition to patch clamp, alternative loading experiments such as nanoindentation (8,74) can be explored. Finally, the interaction between multiple MS channels in a vesicle can be rather different from the equi-biaxial tension case presented in Section 5.3, since the stress resulted from channel interaction is superimposed with that generated from complex vesicle geometry and loading mode.

6. Future Look and Improvements of the Continuum Mechanics Framework

6.1. Future improvements

There is plenty of room for improving the continuum mechanics framework. In essence, the model can be systematically made more realistic by incorporating additional refinements in terms of both structural features of the protein/membrane and simulation protocols.

For example, a more sophisticated model of protein can be adopted. In Figure 10a, the molecular structure of a subunit (containing TM1/TM2/S1/S2/S3 helices and loops) of *E. coli*-MscL is shown. With the main chain of protein helices treated as a cluster of cylindrical cylinders (as in the present MDeFEM model, Figure 1), it is difficult to calculate the contribution of solvation. With respect to Figure 10a, the real helices have irregular atomic “surfaces” dominated by side chain atoms that interact extensively with each other as well as with the surrounding solvent/lipids. Therefore, a more realistic protein model should reflect its surface topology; an example of such an improved model of the MscL subunit is given in Figure 10b, which describes the solvent accessible surface area (SASA) (75) with meshed 3D elements. The similar model has been used by Bathe to study low frequency normal modes of large protein systems (76). The availability of SASA allows one to couple continuum mechanics and continuum solvation models (e.g. the Poisson-Boltzmann (PB) (77), Generalized Born (GB) (78), or other implicit methods(79)) to describe protein structural transition under the influence of solvent. It is suspected that the solvation term can cause local lipid membrane bending, thereby reduce the external membrane strain required for gating (which was unrealistically large in (8)).

Besides incorporating the actual morphology of biomolecules, more sophisticated parameterization procedures can be adopted. For helices, a critical improvement underway is to treat them as heterogeneous (e.g. sequence-dependent) and anisotropic. Such improvement is required to study helix kinking, which has been proposed to play an important role in the gating transition of several channels (80); handling unfolding events of helices and other secondary structural elements, which have been proposed as part of many large-scale conformational transitions (81), is more challenging at the continuum level and will be an

important subject of research. For lipid, anisotropic properties are necessary to model the membrane in a more realistic fashion; e.g., lipid membrane is unable to bear in-plane shear deformation, and this phenomenological behavior can be modeled using the transverse isotropic material description. In addition, local residual stress and curvature, as well as hyperelastic and time-dependent viscoelastic features of lipid provide ways to avoiding excessive strain and stress required by the current solid slab membrane model (7). Although the solid slab lipid model is a major approximation in the continuum-based MDeFEM approach, we have shown that it can nevertheless effectively describe the appropriate expansion of lipid cavity that is needed to accommodate the full gating of MscL upon equi-biaxial tension. The elastic model was also able to predict a critical channel separation for co-operativity in qualitative agreement with ref. (49), despite the fact that the tension is not uniformly distributed in the solid membrane while stress distribution in realistic membrane is largely uniform.

The interactions among continuum components can also be described more realistically. Different interaction parameters can be assigned to hydrophilic and hydrophobic surface regions of protein/lipid, which helps to properly anchor the protein in the membrane. The lateral interaction component can also be incorporated, which is able to stabilize the system and help create local free energy minima during the gating transition (i.e. making certain intermediate states more stable). Such refinement, along with the incorporation of solvation, could effectively create locally stabilizing wells and barriers and make the continuum model more realistic.

Finally, explicit time-dependence in the continuum simulation at a constant temperature can be introduced in the framework of Langevin dynamics as commonly done in particle based simulations (82). Introducing thermal fluctuations is essential to making the gating process more realistic, such as the asymmetry between the motions of different subunits discussed in recent experimental and simulation studies (20,46,56,83). It is also expected that the employment of electrical field/external charges could also affect the gating behaviors (84, 85), in addition to mechanical loads.

6.2. Potential application of MDeFEM to other channel systems

The MDeFEM simulations have so far focused on MscL because of its relatively simple structural topology and extensive experimental background. Once calibrated, the MDeFEM framework can be applied to other MS channels that are less understood. For example, many TRP channels, which have attracted much attention in recent years due to their diverse roles in important physiological functions (86,87), have mechanosensitivity. Sequence analysis of a specific system analyzed recently (88,89) indicates that the structure is likely similar to that of the voltage-gated potassium *Shaker* channel. Although the structural response of MscL during gating is very global in nature, the gating transition of the *Shaker* channel is believed to be dependent on rather local interactions and conformational transitions (90–92). In addition, although MscL is mostly mechanosensitive, many TRP channels are known to be “poly-modal” and can be activated by several different forms of stimuli (86,87). Therefore, it is interesting to explore whether fundamentally different mechano-sensing mechanisms are operational in these systems or there are common features, and to identify sequence/structural/energetic features that dictate the variations in the gating characteristics.

Another MS channel that attracted much attention is the mechanosensitive channel of small conductance (MscS). MscS has homologues in many species and has a much wider distribution than MscL. Although an x-ray structure of MscS (93) has been solved, the functional mechanism of this channel remains largely unclear. Indeed, even the identity of the x-ray structure has been controversial; the relatively large pore radius led the crystallographers (93) conclude that the structure represents an open state of the channel, while the opposite

conclusion was reached based on drying transitions observed in the MD simulations (94). More recent MD simulation argued that the x-ray structure is capable of transport once the transmembrane potential is present (95,96), although transmembrane potentials much larger than that found under physiology condition had to be used to observe transport. The gating process of MscS is more complex than that of MscL in that it is not only activated by membrane tension but is also modulated by voltage and has a rather complex inactivation mechanism under sustained stimulus (97–100). Moreover, a recent study (99) found that the gating behavior of MscS is even sensitive to the rate of stimulation; it is fully responsive to sudden change in tension but unresponsive to slowly applied tension. These complex features of MscS and the difficulties associated with a direct experimental analysis of the interplay between membrane tension and transmembrane voltage make a computational analysis highly worthwhile. Since the opening of MscS is also enhanced by the addition of lysophosphatidylcholine and other amphipaths (101), it is likely that the basic MDeFEM framework established in the MscL study is also applicable.

7. Conclusion

In this review, recent advances in the mechanistic understanding of gating transitions in mechanosensitive channels are summarized. We mainly focus on insights derived from a continuum-mechanics based approach (MDeFEM) in the study of a widely studied MS channel, the *E. coli*-MscL. Although the model is clearly in its infancy and needs to be improved for quantitative analysis, its initial application has successfully demonstrated that mechanics principles play an important role in governing the conformational response of the MS channel to external mechanical perturbation in the membrane (8). We believe that many of these mechanical principles are likely to play a role in various membrane mediated biomechanical processes. The advantage, limitation, and future improvements of the continuum-mechanics based approach are discussed. Being top-down in nature, the molecular dynamics-decorated finite element method (MDeFEM) complements rather than competes with the traditional bottom-up all-atom/coarse-grained simulations (62–65). While the particle based coarse-grained models are better suited for investigating mechanistic issues involving near-atom scales, such as the role of protein/lipid interactions in the gating of MS channels, the MDeFEM approach is particularly useful for studying processes that involve large-scale deformations and complex mechanistic perturbations. In fact, coarse-grained particle simulations can be used to generate some key properties required in the MDeFEM model as well as testing the reliability of MDeFEM simulations.

With the experience in applying the continuum framework to MscL and continued efforts in refining the versatile MDeFEM approach, similar studies can be made to systems that remain poorly understood, especially those with complex geometry and mechanical loads that are not accessible to standard particle based simulations. The multiscale framework can also be applied to study the gating mechanisms of different types of ion channels upon various external stimuli, such as comparing the gating characteristics of the *Shaker* potassium channel (86,87) to MscL, and the MS channel of small conductance (MscS) (68) to identify unique structural and energetic features of mechanosensitive channels. It is envisioned that these studies will lead to further exciting researches to uncover the basic principles of mechanosensations, mechanotransductions and other mechanobiological processes.

Acknowledgements

The work of YT and XC are supported by NSF CMS-0407743 and CMMI-0643726. The work of JY and QC are supported by the National Institutes of Health (R01-GM071428). QC also acknowledges a Research Fellowship from the Alfred P. Sloan Foundation. Computational resources from the National Center for Supercomputing Applications at the University of Illinois are greatly appreciated.

References

1. Hamill OP, Martinac B. Molecular basis of mechanotransduction in living cells. Physiological Reviews 2001;81:685–740. [PubMed: 11274342]
2. Ingber DE. Cellular mechanotransduction: putting all the pieces together again. Faseb Journal 2006;20:811–827. [PubMed: 16675838]
3. Kamm RD, Kaazempur-Mofrad MR. On the molecular basis for mechanotransduction. Mech Chem Biosyst 2004;1:201–9. [PubMed: 16783933]
4. Martinac B. Mechanosensitive ion channels: molecules of mechanotransduction. Journal of Cell Science 2004;117:2449–2460. [PubMed: 15159450]
5. Bounoutas A, Chalfie M. Touch sensitivity in Caenorhabditis elegans. Pflugers Archiv-European Journal of Physiology 2007;454:691–702. [PubMed: 17285303]
6. Tang Y, Cao G, Chen X, Yoo J, Yethiraj A, Cui Q. A finite element framework for studying the mechanical response of macromolecules: Application to the gating of the mechanosensitive channel MscL. Biophysical Journal 2006;91:1248–1263. [PubMed: 16731564]
7. Chen X, Cui Q, Yoo J, Tang Y, Yethiraj A. Gating mechanisms of the mechanosensitive channels of large conductance, Part I: Theoretical and Numerical Framework. Biophysical Journal 2008;95:563–580. [PubMed: 18390626]
8. Tang Y, Yoo J, Yethiraj A, Cui Q, Chen X. Gating Mechanisms of Mechanosensitive Channels of Large Conductance Part II: Systematic Study of Conformational Transitions. Biophysical Journal 2008;95:581–596. [PubMed: 18390625]
9. Gustin MC, Zhou XL, Martinac B, Kung C. A mechanosensitive ion channel in the yeast plasma-membrane. Science 1988;242:762–765. [PubMed: 2460920]
10. Kernan MJ. Mechanotransduction and auditory transduction in Drosophila. Pflugers Archiv-European Journal of Physiology 2007;454:703–720. [PubMed: 17436012]
11. Makino A, Prossnitz ER, Bunemann M, Wang JM, Yao WJ, Schmid-Schoenbein GW. G protein-coupled receptors serve as mechanosensors for fluid shear stress in neutrophils. American Journal of Physiology-Cell Physiology 2006;290:C1633–C1639. [PubMed: 16436471]
12. Chang G, Spencer RH, Lee AT, Barclay MT, Rees DC. Structure of the MscL homolog from Mycobacterium tuberculosis: A gated mechanosensitive ion channel. Science 1998;282:2220–2226. [PubMed: 9856938]
13. Sukharev S, Betanzos M, Chiang CS, Guy HR. The gating mechanism of the large mechanosensitive channel MscL. Nature 2001;409:720–724. [PubMed: 11217861]
14. Sukharev S, Anishkin A. Mechanosensitive channels: what can we learn from ‘simple’ model systems? Trends in Neurosciences 2004;27:345–351. [PubMed: 15165739]
15. Sukharev S, Durell SR, Guy HR. Structural models of the MscL gating mechanism. Biophysical Journal 2001;81:917–936. [PubMed: 11463635]
16. Sukharev SI, Sigurdson WJ, Kung C, Sachs F. Energetic and spatial parameters for gating of the bacterial large conductance mechanosensitive channel, MscL. Journal of General Physiology 1999;113:525–539. [PubMed: 10102934]
17. Sukharev SI, Blount P, Martinac B, Blattner FR, Kung C. A Large-Conductance Mechanosensitive Channel in E. Coli Encoded by Mscl Alone. Nature 1994;368:265–268. [PubMed: 7511799]
18. Wiggins P, Philips R. Analytical models for mechanotransduction: Gating a mechanosensitive channel. Proceedings of the National Academy of Sciences of the United States of America 2004;101:4071–4076. [PubMed: 15024097]
19. Kloda A, Martinac B. Mechanosensitive channel of Thermoplasma, the cell wall-less Archaea - Cloning and molecular characterization. Cell Biochemistry and Biophysics 2001;34:321–347. [PubMed: 11898860]
20. Perozo E, Kloda A, Cortes DM, Martinac B. Physical principles underlying the transduction of bilayer deformation forces during mechanosensitive channel gating. Nature Structural Biology 2002;9:696–703.
21. Moe P, Blount P. Assessment of potential stimuli for mechano-dependent gating of mscl: effects of pressure, tension and lipid headgroups. Biochem 2005;44:12239–12244. [PubMed: 16142922]

22. Gullingsrud J, Schulten K. Lipid bilayer pressure profiles and mechanosensitive channel gating. Biophysical Journal 2004;86:3496–3509. [PubMed: 15189849]
23. Elmore DE, Dougherty DA. Investigating Lipid Composition Effects on the Mechanosensitive Channel of Large Conductance (MscL) Using Molecular Dynamics Simulations. Biophys J 2003;85:1512–1524. [PubMed: 12944269]
24. Nagle JF, Tristram-Nagle S. Structure of lipid bilayers. Biochimica Et Biophysica Acta-Reviews on Biomembranes 2000;1469:159–195.
25. Evans E, Hochmuth R. Mechanical properties of membranes. Topics in membrane and transport 1978;10:1–64.
26. Turner MS, Sens P. Gating-by-tilt of mechanically sensitive membrane channels. Phys Rev Lett 2004;93:118103. [PubMed: 15447384]
27. Lindahl E, Edholm O. Spatial and energetic-entropic decomposition of surface tension in lipid bilayers from molecular dynamics simulations. J Chem Phys 2000;113:3882–3893.
28. Perozo E. Gating prokaryotic mechanosensitive channels. Nature Reviews Molecular Cell Biology 2006;7:109–119.
29. Kung C. A possible unifying principle for mechanosensation. Nature 2005;436:647–654. [PubMed: 16079835]
30. Markin VS, Sachs F. Thermodynamics of mechanosensitivity: lipid shape, membrane deformation and anesthesia. Biophysical Journal 2004;86:370A–370A.
31. Wiggins P, Philips R. Membrane-protein interactions in mechanosensitive channels. Biophys J 2005;88:880–902. [PubMed: 15542561]
32. Martinac B, Buechner M, Delcour AH, Adler J, Kung C. Pressure-Sensitive Ion Channel in Escherichia-Coli. Proceedings of the National Academy of Sciences of the United States of America 1987;84:2297–2301. [PubMed: 2436228]
33. Sukharev SI, Blount P, Martinac B, Kung C. Mechanosensitive channels of Escherichia coli: The MscL gene, protein, and activities. Annual Review of Physiology 1997;59:633–657.
34. Anishkin A, Gendel V, Sharifi NA, Chiang CS, Shirinian L, Guy HR, Sukharev S. On the conformation of the COOH-terminal domain of the large mechanosensitive channel MscL. Journal of General Physiology 2003;121:227–244. [PubMed: 12601086]
35. Perozo E, Rees D. Structure and mechanism in prokaryotic mechanosensitive channels. Curr Opin Struct Biol 2003;13:432–442. [PubMed: 12948773]
36. Steinbacher S, Strop RBP, Rees DC. Structures of the prokaryotic mechanosensitive channels MscL and MscS. Current Topics in Membranes 2007;58:1–24.
37. Maurer JA, Elmore DE, Clayton D, Xiong L, Lester HA, Dougherty DA. Confirming the Revised C-Terminal Domain of the MscL Crystal Structure. Biophys J 2008;94:4662 – 4667. [PubMed: 18326638]
38. Kloda A, Ghazi A, Martinac B. C-Terminal Charged Cluster of MscL, RKKEE, Functions as a pH Sensor. Biophys J 2006;90:1992–1998. [PubMed: 16387769]
39. Blount P, Sukharev SI, Moe PC, Nagle SK, Kung C. Towards an understanding of the structural and functional properties of MscL, a mechanosensitive channel in bacteria. Biology of the Cell 1996;87:1–8. [PubMed: 9004483]
40. Gu LQ, Liu WH, Martinac B. Electromechanical coupling model of gating the large mechanosensitive ion channel (MscL) of Escherichia coli by mechanical force. Biophysical Journal 1998;74:2889–2902. [PubMed: 9635742]
41. Yoshimura K, Batiza A, Schroeder M, Blount P, Kung C. Hydrophilicity of a single residue within MscL correlates with increased channel mechanosensitivity. Biophysical Journal 1999;77:1960–1972. [PubMed: 10512816]
42. Yoshimura K, Nomura T, Sokabe M. Loss-of-Function Mutations at the Rim of the Funnel of Mechanosensitive Channel MscL. Biophys J 2004;86:2113–2120. [PubMed: 15041651]
43. Anishkin A, Chiang CS, Sukharev S. Gain of function mutations reveal expanded intermediate states and a sequential action of two gates in mscl. J Gen Physiol 2005;125:155–170. [PubMed: 15684093]

44. Ajouz B, Berrier C, Besnard M, Martinac B, Ghazi A. Contributions of the different extramembranous domains of the mechanosensitive ion channel MscL to its response to membrane tension. J Biol Chem 2000;275:1015–1022. [PubMed: 10625640]
45. Park KH, Berrier C, Martinac B, Ghazi A. Purification and functional reconstitution of N- and C-halves of the MscL channel. Biophys J 2004;86:2129–2136. [PubMed: 15041653]
46. Perozo E, Cortes DM, Sompornpisut P, Kloda A, Martinac B. Open channel structure of MscL and the gating mechanism of mechanosensitive channels. Nature 2002;418:942–948. [PubMed: 12198539]
47. Corry B, Rigby P, Liu ZW, Martinac B. Conformational changes involved in MscL channel gating measured using FRET spectroscopy. Biophysical Journal 2005;89:L49–L51. [PubMed: 16199508]
48. Blount P, Schroeder MJ, Kung C. Mutations in a bacterial mechanosensitive channel change the cellular response to osmotic stress. J Biol Chem 1997;272:32150–32157. [PubMed: 9405414]
49. Ursell T, Huang KC, Peterson E, Phillips R. Cooperative gating and spatial organization of membrane proteins through elastic interactions. Plos Computational Biology 2007;3:803–812.
50. Tirion MM. Low amplitude motions in proteins from a single-parameter atomic analysis. Phys Rev Lett 1996;77:1905–1908. [PubMed: 10063201]
51. Valadie H, Lacapcre JJ, Sanejouand YH, Etchebest C. Dynamical properties of the MscL of Escherichia coli: a normal mode analysis. J Mol Biol 2003;332:657–674. [PubMed: 12963374]
52. Ikeguchi M, Ueno J, Sato M, Kidera A. Protein Structural Change Upon Ligand Binding: Linear Response Theory. Phys Rev Lett 2005;94:078102. [PubMed: 15783858]
53. Karplus M, McCammon JA. Molecular dynamics simulations of biomolecules (vol 9, pg 646, 2002). Nature Structural Biology 2002;9:788–788.
54. Gullingsrud J, Schulten K. Gating of MscL studied by steered molecular dynamics. Biophysical Journal 2003;85:2087–2099. [PubMed: 14507677]
55. Gullingsrud J, Kosztin D, Schulten K. Structural determinants of MscL gating studied by molecular dynamics simulations. Biophysical Journal 2001;80:2074–2081. [PubMed: 11325711]
56. Jeon J, Voth GA. Gating of the Mechanosensitive Channel Protein MscL: The Interplay of Membrane and Protein. Biophysical Journal 2008;94:3497–3511. [PubMed: 18212020]
57. Schlitter J, Engels M, Kruger P, Jacoby E, Wollmer A. Targeted molecular-dynamics simulation of conformational change - application to the T$R transition insulin. Molecular Simulation 1993;10:291–308.
58. Kong YF, Shen YF, Warth TE, Ma JP. Conformational pathways in the gating of Escherichia coli mechanosensitive channel. Proceedings of the National Academy of Sciences of the United States of America 2002;99:5999–6004. [PubMed: 11972047]
59. Bilston LE, Mylvaganam K. Molecular simulations of the large conductance mechanosensitive (MscL) channel under mechanical loading. Febs Letters 2002;512:185–190. [PubMed: 11852077]
60. Meyer GR, Gullingsrud J, Schulten K, Martinac B. Molecular dynamics study of MscL interactions with a curved lipid bilayer. Biophysical Journal 2006;91:1630–1637. [PubMed: 16751236]
61. Debret G, Valadié H, Stadler AM, Etchebest C. New insights of membrane environment effects on MscL channel mechanics from theoritical approaches. Proteins 2008;71:1183–1196. [PubMed: 18004782]
62. Yefimov S, van der Giessen E, Onck PR, Marrink SJ. Mechanosensitive membrane channels in action. Biophysical Journal 2008;94:2994–3002. [PubMed: 18192351]
63. Shi Q, Izvekov S, Voth GA. Mixed atomistic and coarse-grained molecular dynamics: simulation of a membrane-bound ion channel. J Phys Chem B 2006;110:15045–15048. [PubMed: 16884212]
64. Marrink SJ, Risselada HJ, Yefimov S, Tieleman DP, Vries AHd. The MARTINI forcefield: coarse-grained model for biomolecular simulations. J Phys Chem B 2007;111:7812–7824. [PubMed: 17569554]
65. Lopez CF, Nielsen SO, Moore PB, Klein ML. Understanding nature's design for a nanosyringe. Proc Natl Acad Sci USA 2004;101:4431–4434. [PubMed: 15070735]
66. Izvekov S, Voth GA. Multiscale coarse graining of liquid-state systems. J Chem Phys 2005;123:134105. [PubMed: 16223273]
67. ABAQUS. Abaqus 6.4 user's manual. ABAQUS Inc.; 2004.

68. Anishkin A, Kung C. Microbial mechanosensation. Current Opinion in Neurobiology 2005;15:397–405. [PubMed: 16006117]
69. Ling CB. On the stresses in a plate containing 2 circular holes. Journal of Applied Physics 1948;19:77–81.
70. Hamill OP, Marty A, Neher E, Sakmann B, Sigworth FJ. Improved patch-clamp techniques for high-resolution current recording from cells and cell-free membrane patches. Pflugers Arch 1981;391:85–100. [PubMed: 6270629]
71. Sachs F, Morris CE. Mechanosensitive ion channels in nonspecialized cells. Rev Physiol Biochem Pharmacol 1998;132:1–77. [PubMed: 9558913]
72. Hamill OP, Martinac B. Molecular basis of mechanotransduction in living cells. Physiol Rev 2001;81:685–740. [PubMed: 11274342]
73. Hartmann C, Delgado A. Stress and strain in a yeast cell under high hydrostatic pressure. PAMM 2004;4:316–317.
74. Gordon VD, Chen X, Hutchinson JW, Bausch AR, Marquez M, Weitz DA. Self-assembled polymer membrane capsules inflated by osmotic pressure. Journal of the American Chemical Society 2004;126:14117–14122. [PubMed: 15506776]
75. Sanner, M. 2008. Http://Www.Scripps.Edu/~Sanner/Html/Msms_Home.Html
76. Bathe M. A finite element framework for computation of protein normal modes and mechanical response. Proteins-Structure Function and Bioinformatics 2008;70:1595–1609.
77. Baker NA, Sept D, Joseph S, Holst MJ, McCammon JA. Electrostatics of nanosystems: Application to microtubules and the ribosome. Proceedings of the National Academy of Sciences of the United States of America 2001;98:10037–10041. [PubMed: 11517324]
78. Feig M, Brooks CL. Recent advances in the development and application of implicit solvent models in biomolecule simulations. Current Opinion in Structural Biology 2004;14:217–224. [PubMed: 15093837]
79. Zhou YC, Holst M, McCammon JA. A nonlinear elasticity model of macromolecular conformational change induced by electrostatic forces. Journal of Mathematical Analysis and Applications 2008;340:135–164.
80. Akitake B, Anishkin A, Liu N, Sukharev S. Straightening and sequential buckling of the pore-lining helices define the gating cycle of MscS. Nature Structural & Molecular Biology 2007;14:1141–1149.
81. Miyashita O, Onichic JN, Wolynes PG. Nonlinear elasticity, proteinquakes, and the energy landscapes of functional transitions in proteins. Proc Natl Acad Sci USA 2003;100:12570–12575. [PubMed: 14566052]
82. Zwanzig, R. Non-Equilibrium Statistical Mechanics. New York: Oxford University Press; 2001.
83. Iscla IGL, Wray R, Blount P. Disulfide Trapping the Mechanosensitive Channel MscL into a Gating-Transition State. Biophysical Journal 2007;92:1224–1232. [PubMed: 17114217]
84. Liu L, Qiao Y, Chen X. Pressure-Driven Water Infiltration into Carbon Nanotube: The Effect of Applied Charges. Applied Physics Letters 2008;92:101927.
85. Han A, Chen X, Qiao Y. Effects of Addition of Electrolyte on Liquid Infiltration in a Hydrophobic Nanoporous Silica Gel. Langmuir 2008;24:7044–7047. [PubMed: 18564859]
86. Ramsey IS, Delling M, Clapham DE. An introduction to TRP channels. Annu Rev Physiol 2006;68:619–647. [PubMed: 16460286]
87. Dhaka A, Viswanath V, Patapoutian A. TRP ion channels and temperature sensation. Annu Rev Neurosci 2006;29:135–161. [PubMed: 16776582]
88. Zhou X, Batiza AF, Loukin SH, Palmer CP, Kung C, Saimi Y. The transient receptor potential channel on the yeast vacuole is mechanosensitive. Proc Natl Acad Sci USA 2003;100:7105–7110. [PubMed: 12771382]
89. Saimi Y, Zhou XL, Loukin SH, Haynes WJ, Kung C. Microbial TRP channels and their mechanosensitivity. Mechanosensitive Ion Channels, Part A 2007:311–327.
90. Tombola F, Pathak MM, Isacoff EY. How does voltage open an ion channel. Annu Rev Cell Dev Biol 2006;22:23–52. [PubMed: 16704338]
91. Long SB, Campbell EB, MacKinnon R. Crystal structure of a mammalian voltage-dependent Shaker family K+ channel. Science 2005;309:897–903. [PubMed: 16002581]

92. Long SB, Campbell EB, MacKinnon R. Voltage sensor of kv1.2: Structural basis of electromechanical coupling. Science 2005;309:903–908. [PubMed: 16002579]

93. Bass RB, Strop P, Barclay MT, Rees DC. Crystal structure of Escherichia coli MscS, a voltage-modulated and mechanosensitive channel. Science 2002;298:1582–1587. [PubMed: 12446901]

94. Anishkin A, Sukharev S. Water dynamics and dewetting transition in the small mechanosensitive channel MscS. Biophysical Journal 2004;86:2883–2895. [PubMed: 15111405]

95. Spronk SA, Elmore DE, Dougherty DA. Voltage-dependent hydration and conduction properties of the hydrophobic pore of the mechanosensitive channel of small conductance. Biophysical Journal 2006;90:3555–3569. [PubMed: 16500980]

96. Sotomayor M, Vasquez V, Perozo E, Schulten K. Ion conduction through MscS as determined by electrophysiology and simulation. Biophysical Journal 2007;92:886–902. [PubMed: 17114233]

97. Edwards MD, Booth IR, Miller S. Gating the bacterial mechanosensitive channels: MscS a new paradigm? Curr Opin Micro 2004;7:163–167.

98. Edwards MD, Li Y, Kim S, Miller S, Bartlett W, Black S, Dennison S, Iscla I, Blount P, Bowie JU, Booth IR. Pivotal role of the glycine-rich TM3 helix in gating the MscS mechanosensitive channel. Nat Struct Mol Biol 2005;12:113–119. [PubMed: 15665866]

99. Akitake B, Anishkin A, Sukharev S. The “dashpot” mechanism of stretch-dependent gating in MscS. J Gen Physiol 2005;125:143–154. [PubMed: 15657299]

100. Perozo E. Gating Prokaryotic mechanosensitive channels. Nat Rev Mol Cell Biol 2006;7:109–119. [PubMed: 16493417]

101. Martinac B, Adler J, Kung C. Mechanosensitive ion channels of E. coli activated by amphipaths. Nature 1990;348:261–263. [PubMed: 1700306]

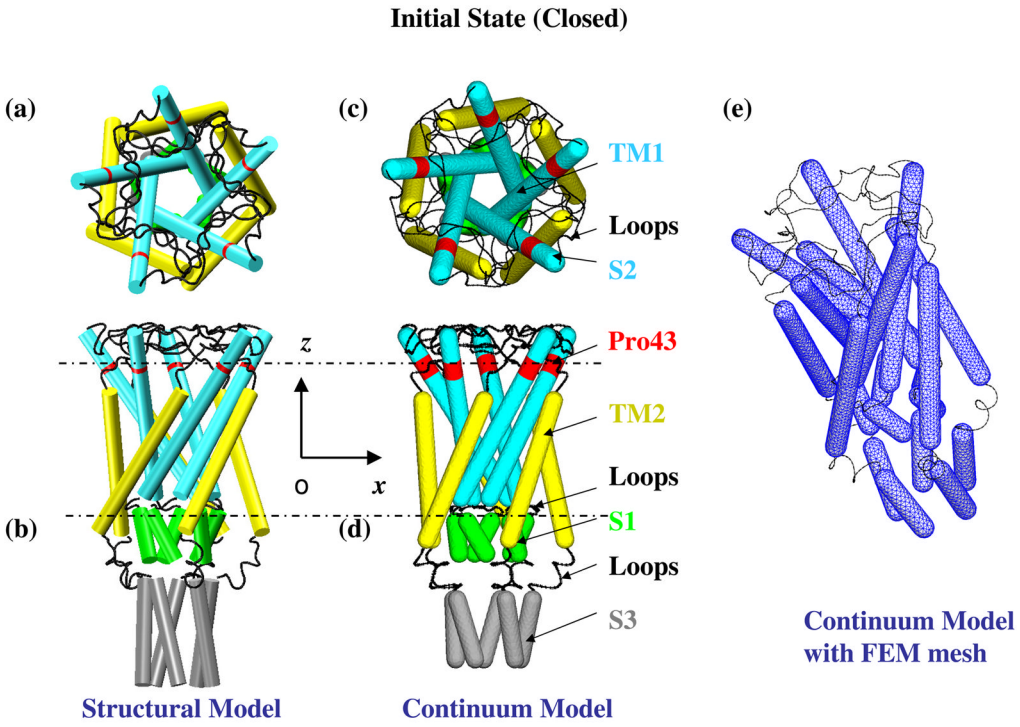

Fig. 1.

E. coli-MscL: (a) top view and (b) side view of the closed structure of the homology model (14) (c) top view and (d) side view of the MDeFEM model; (e) mesh of the protein. The dash line indicates the initial location of lipid membrane. The protein components include: the transmembrane TM1 bundle (sky blue) and TM2 subunits (yellow), cytoplasmic S1 helices (green) and S3 helices (grey), and they are connected by periplasmic and cytoplasmic loops (black).

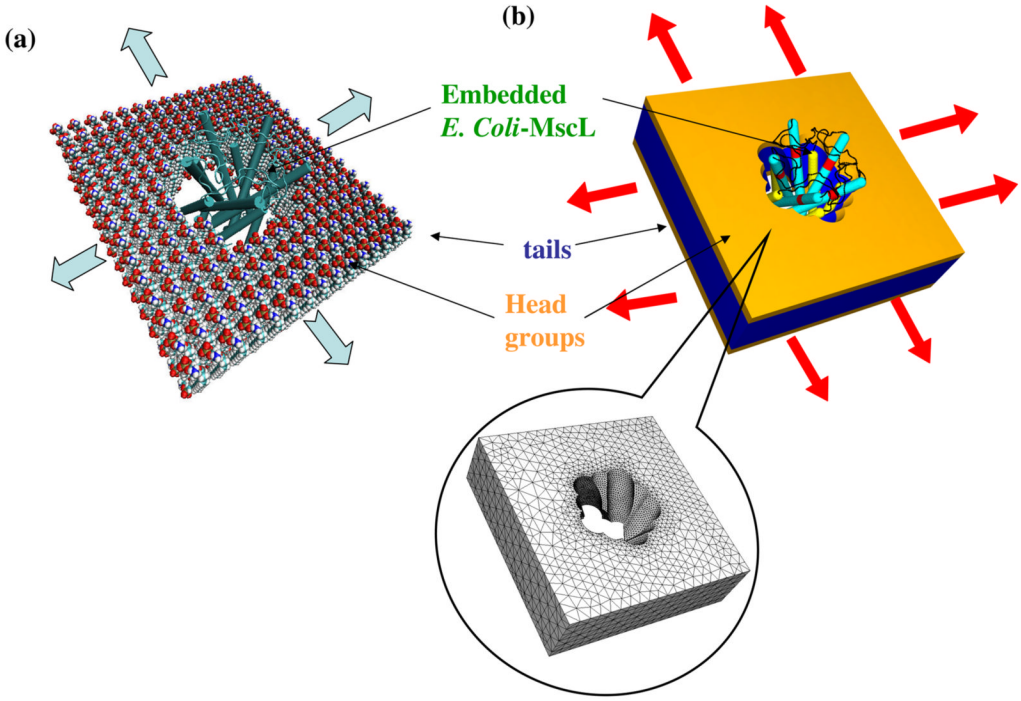

Fig. 2.

The assembled protein/lipid system: (a) the "cartoon" representation of *E. coli*-MscL and all-atom representation of a lipid, with a schematic of equi-biaxial loading applied at the lipid boundary. (b) continuum-mechanics based model of the *E. coli*-MscL-lipid system. The finite element mesh of the tri-layer lipid is shown in the zoomed-in view. The integrated protein structure (established from the continuum approach) is embedded in a continuum lipid slab (based on a sandwich model). The effective mechanical properties of the continuum components as well as their interactions are derived from MD simulations (54).

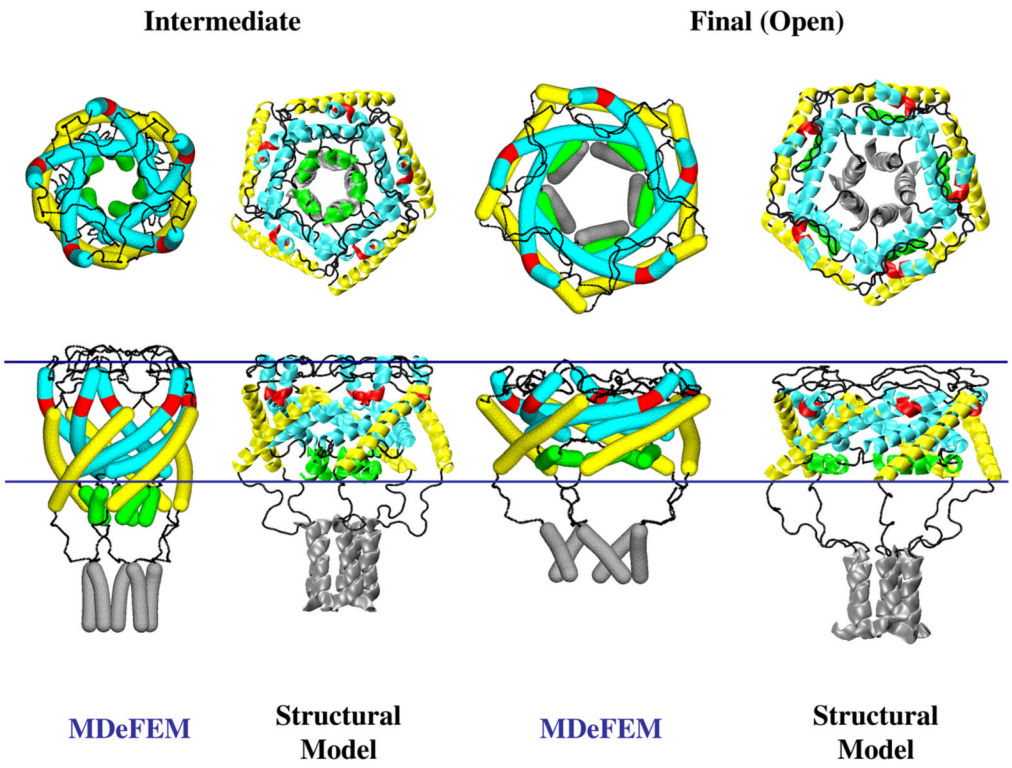

Fig. 3.

Snapshots along the gating pathways of a single *E. coli*-MscL at half- and fully-opened states upon equi-biaxial tension: comparisons between the structural model (14) and MDeFEM simulation (with maximum membrane strain 21%). Gating is primarily realized through the interaction between transmembrane helices and lipid, where the pore enclosed by the TM1 helices (light blue) is pulled open. Other cytoplasmic helices and loops follow the trajectories of the transmembrane helices.

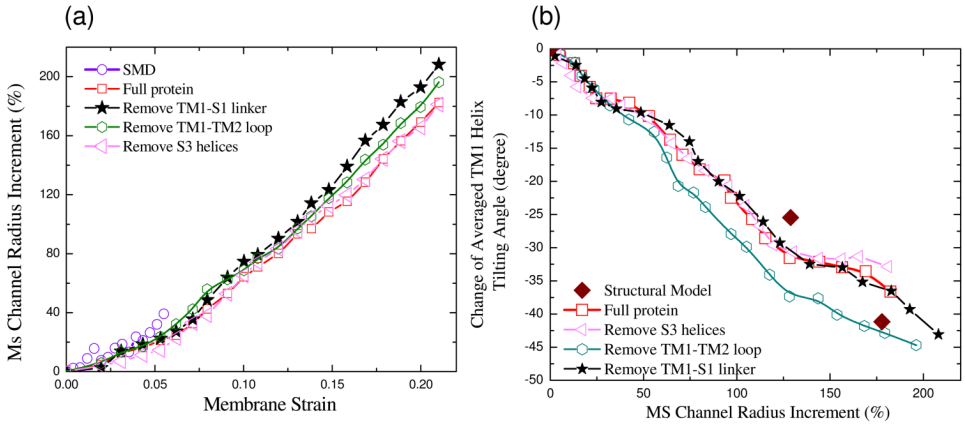

Fig. 4.

Predicted behavior of *E. coli*-MscL upon equi-biaxial tension: (a) the evolution of the effective pore radius (enclosed by TM1 helices) of *E. coli*-MscL versus membrane strain (b) the change of TM1 helix tilting angle as a function of the effective MS channel radius. The results obtained from MDeFEM simulation are compared with those from steered MD simulation (at small strains) and the structural model. In addition, various structural motifs are removed to explore the effect of these protein components during gating.

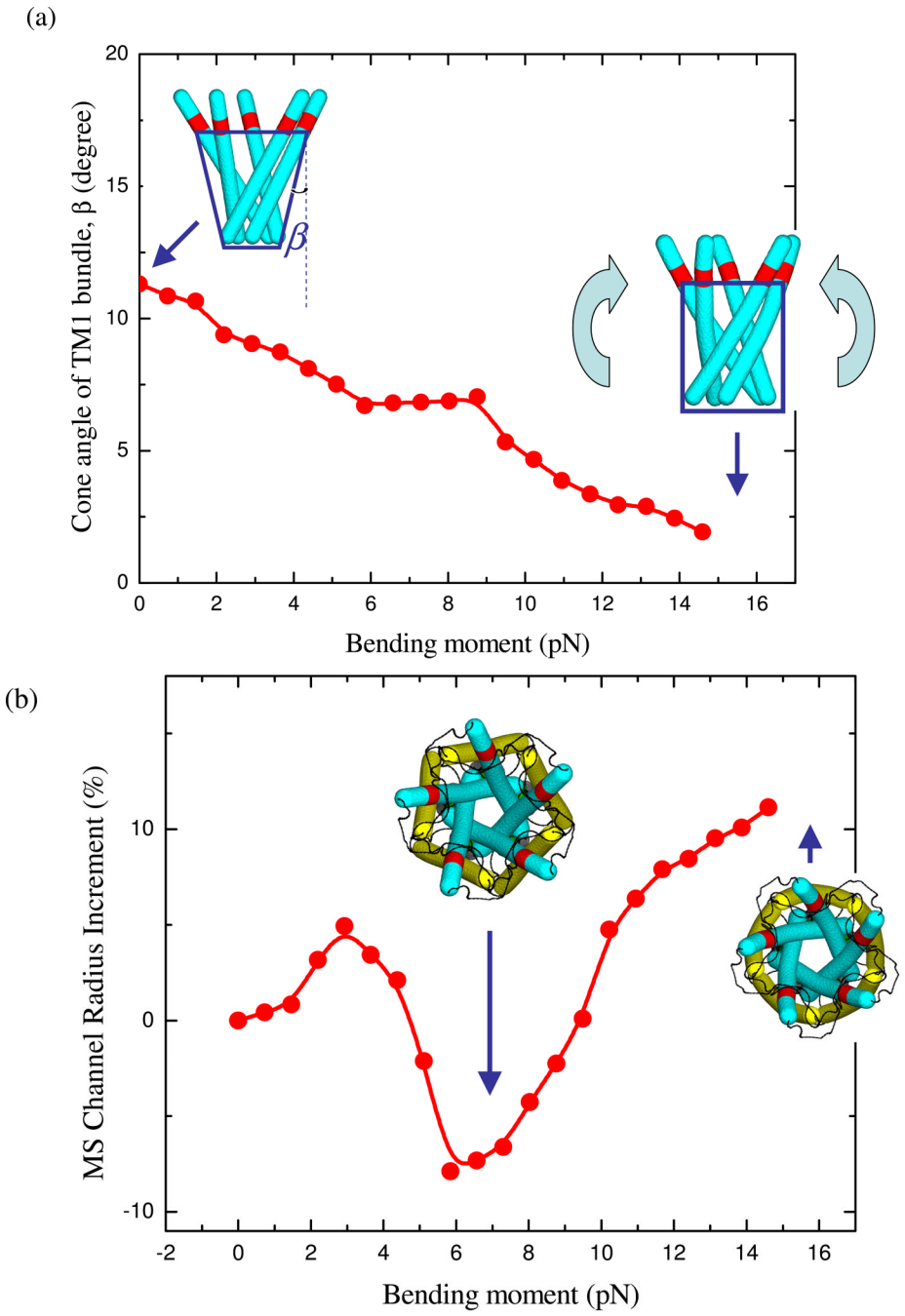

Fig. 5.

Predicted behavior of *E. coli*-MscL upon axisymmetric pure bending as the membrane is bent upwards: (a) change of the TM1 helix bundle cone angle β as a function of the line bending moment, with the inserts showing configurations of the TM1 bundle at different instants (b) increment of the effective pore radius versus the line bending moment, with the inserts showing configurations (top view) of the MscL at different instants.

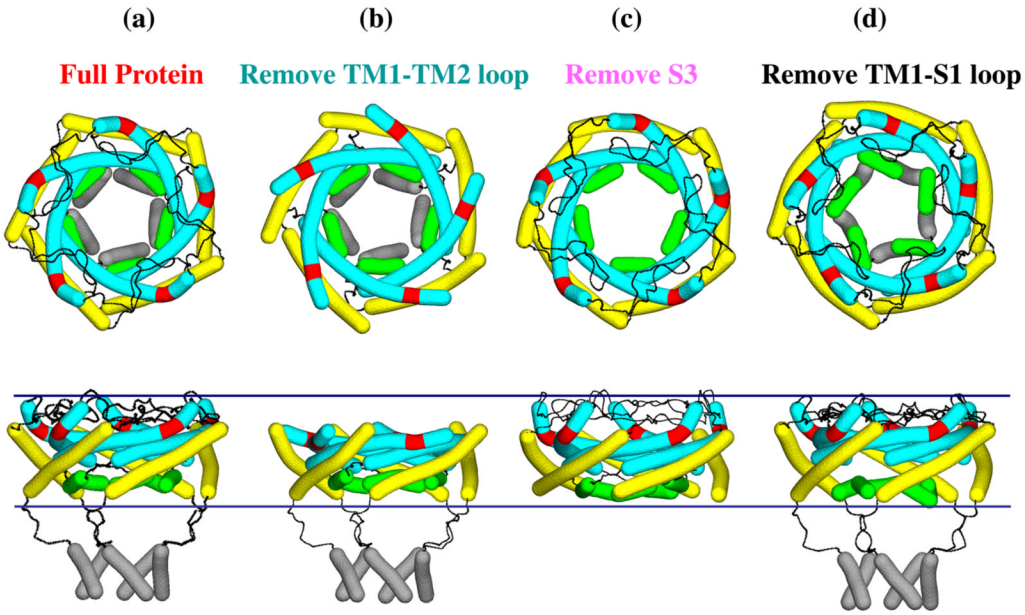

Fig. 6.

Effects of protein structural motifs: (a) Full protein (b) without TM1-TM2-loop (c) without S3 helix bundle (d) without TM1-S1 loop. It is found that moderate structural variations are caused by the removal of the loops, whereas the structural conformation is essentially insensitive to the removal of the S3 bundle. Thus, the continuum simulations show that the S3 bundle plays a relatively minor role during the mechanical gating event whereas the loops constrain gating.

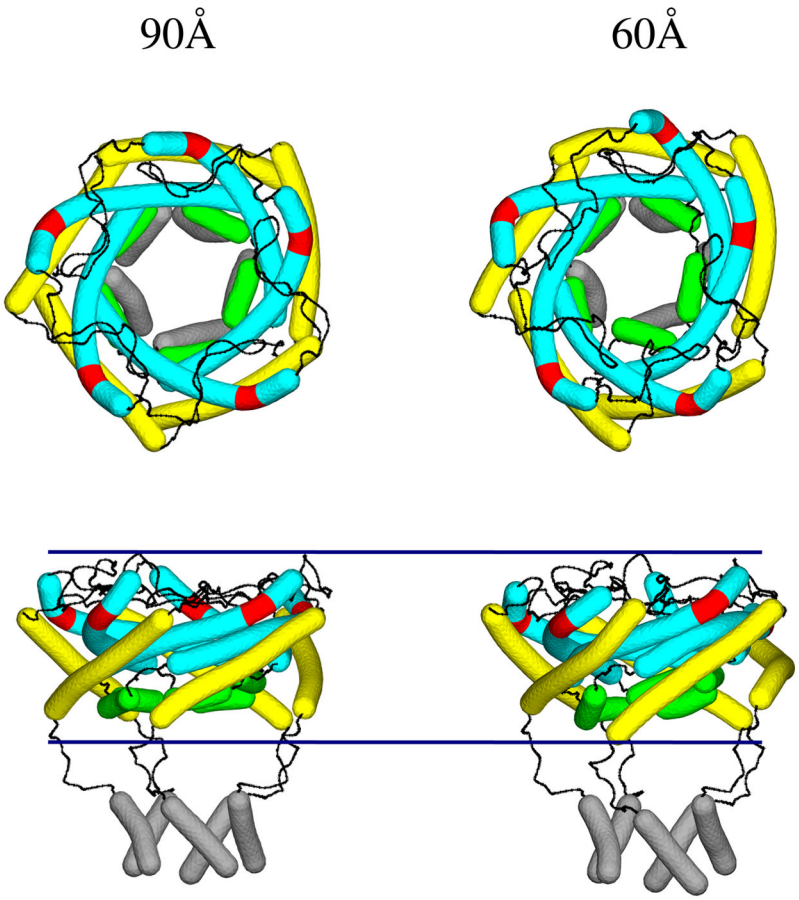

Fig. 7.

The interaction between two *E. coli*-MscLs: the structural configurations of *E. coli*-MscL with the center-to-center separation λ= 90 and 60 Å (at equi-biaxial membrane strain of 21%). The pore enclosed by TM1 helices becomes increasingly distorted as the channel separation is reduced, indicating stronger magnitude of channel interactions.

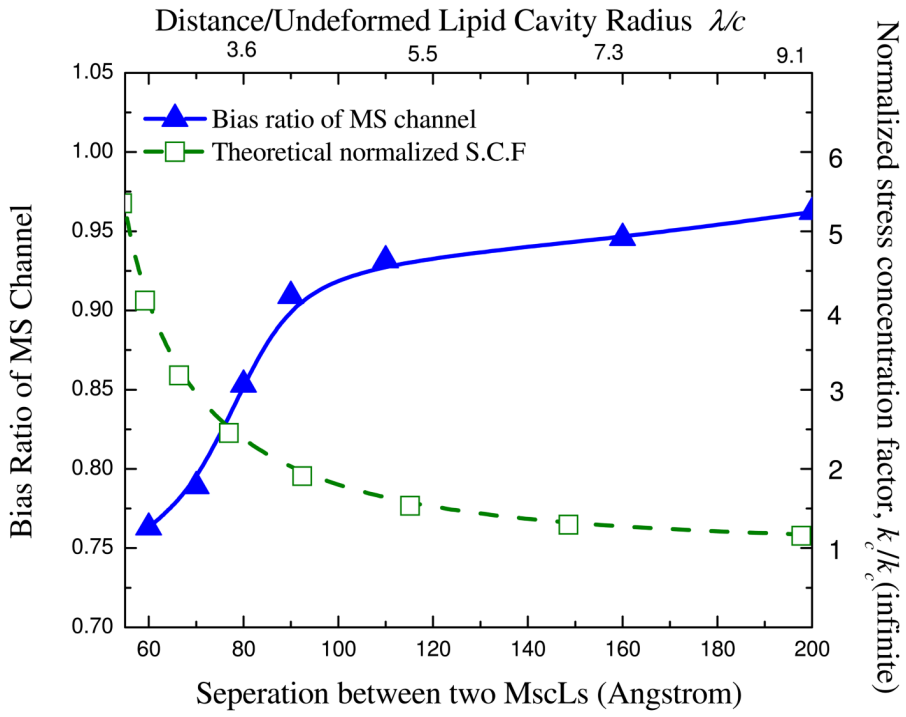

Fig. 8.

Co-operativity between two *E. coli*-MscLs: the bias ratio varies with channel separation, and the results are compared with estimation by elasticity theory (the normalized stress intensity factor, S.C.F., of an elastic sheet containing two circular holes). The bias ratio is the short/long axes ratio of the distorted TM1 pore. The critical separation is about 100 Å below which the two channels strongly interact with each other.

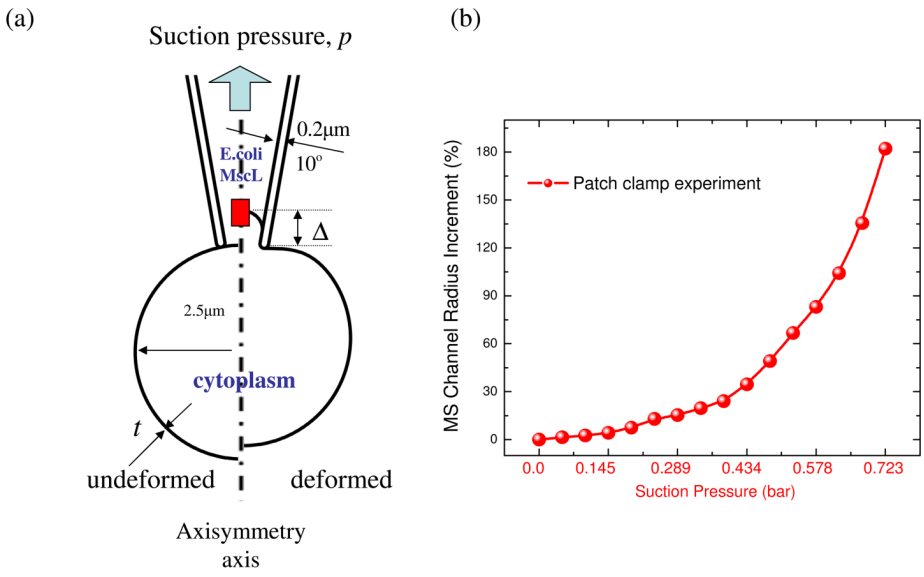

Fig. 9.

Simulation of the patch clamp experiment: (a) schematic of the experiment and location of MscL in the lipid vesicle; undeformed and deformed configurations of the lipid vesicle are compared. (b) Increment of the effective pore radius as a function of the suction pressure (until full gating).

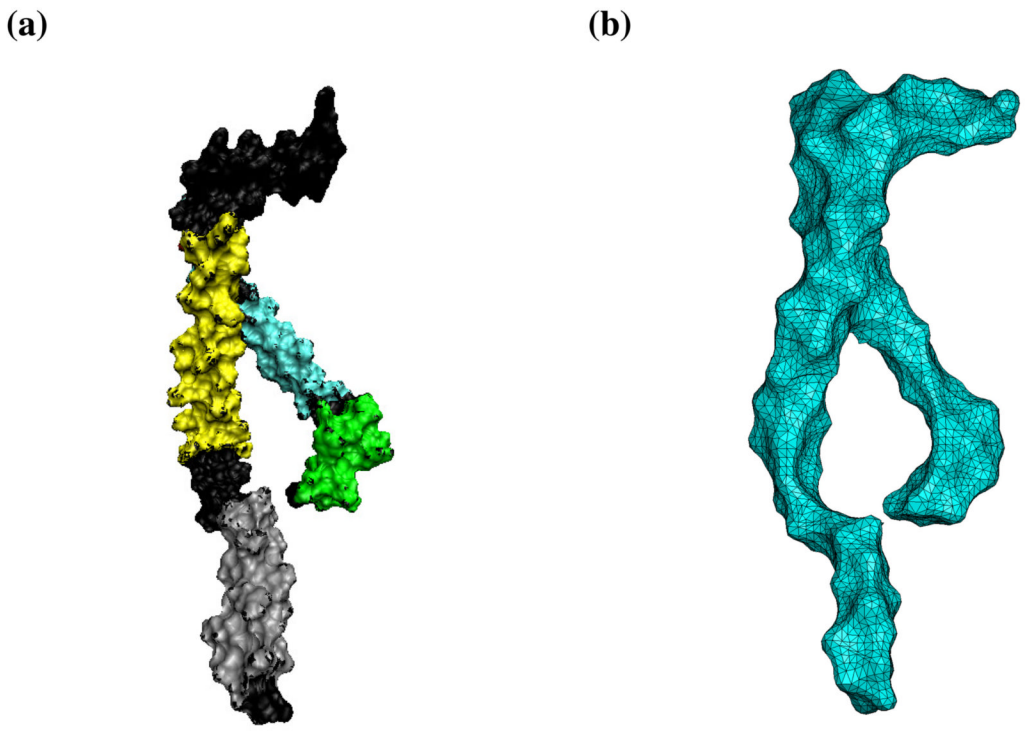

Fig. 10.

A single subunit (TM1/TM2/S1/S2/S3 helices and loops) in *E. coli*-MscL: (a) the solvent accessible surface area (SASA) in molecular representation (b) the finite element mesh of the continuum model. Such representation is useful for calculating solvation forces as an important improvement of the current continuum model.